Picosecond to Microsecond Photodynamics of a Nonplanar Nickel Porphyrin: Solvent Dielectric and Temperature Effects

Charles Michael Drain,[1a,1b] Steve Gentemann,[1a] James A. Roberts,[1a] Nora Y. Nelson,[1c] Craig J. Medforth,[1c] Songling Jia,[1d,1e] M. Cather Simpson,[1d,1f] Kevin M. Smith,[1c] Jack Fajer,[1g] John A. Shelnutt,[1d,1e] and Dewey Holten*,[1a]

Contribution from the Department of Chemistry, Washington University, St. Louis, Missouri 63130, Department of Chemistry, Hunter College of CUNY, 695 Park Avenue, New York, New York 10021, Department of Chemistry, University of California, Davis, California 95616, Materials Theory and Computation Department, Sandia National Laboratories, Albuquerque, New Mexico 87185, Department of Chemistry, University of New Mexico, Albuquerque, New Mexico 87131, Department of Chemistry, Case Western Reserve University, 10900 Euclid Avenue, Cleveland, Ohio 44106, and Department of Applied Science, Brookhaven National Laboratory, Upton, New York 11973

Received December 2, 1997

Abstract: The lifetime of the (d_{z^2},$d_{x^2-y^2}$) metal excited state of nickel(II) 5,10,15,20-tetra-*tert*-butylporphyrin (NiT(*t*-Bu)P) exhibits an extraordinary dependence on solvent dielectric properties and temperature. At room temperature, the excited-state deactivation time varies from 2 ps in highly polar solvents to about 50 ns in nonpolar media. The lifetimes increase to several microseconds in both polar and nonpolar solvents near 80 K. In contrast, the (d,d) lifetimes of nominally planar nickel porphyrins such as nickel tetraphenylporphyrin (NiTPP) vary only weakly with solvent dielectric properties and temperature, and typically fall in the range of 100 to 300 ps. All available evidence indicates that NiT(*t*-Bu)P in solution is highly ruffled (nonplanar) in the ground electronic state. It is proposed that the photoinduced conformational changes that occur in NiT(*t*-Bu)P in order to accommodate the excited-state electronic distribution are limited by the severe steric constraints imposed by the bulky *meso tert*-butyl substituents, and result in molecular and electronic asymmetry and thus a polar excited state. Solvent dielectric properties and temperature modulate these conformational excursions and thus the electronic deactivation rates by affecting the excited-state energies, porphyrin/solvent reorganizations, and the populations of low-frequency out-of-plane vibrations of the macrocycle. The novel findings for this nonplanar nickel porphyrin demonstrate the intimate connectivity that exists between the static and dynamic molecular structures of porphyrins and their ground- and excited-state electronic properties. Furthermore, the results obtained provide insights into the interactions between tetrapyrrole chromophores and their host proteins, and suggest the potential use of nonplanar porphyrins as building blocks for molecular photonics applications.

Introduction

Distortion of tetrapyrrole macrocycles from planarity can be imposed by steric interactions between multiple or bulky peripheral substituents in vitro and between the molecule and the surrounding protein in vivo.[2−5] Such distortions significantly perturb the electronic and vibrational properties of these chromophores.[4−8] The most dramatic effects on photophysical behavior have been found for zinc(II) and free base 5,10,15,20-tetra-*tert*-butylporphyrin, ZnT(*t*-Bu)P and H_2T(*t*-Bu)P.[6b,c] The $^1(\pi,\pi^*)$ excited-state lifetimes (5−50 ps) and fluorescence yields ($(1-5) \times 10^{-4}$) at room temperature are reduced about 200-fold from those of less distorted tetraalkyl analogues such as the *n*-pentyl complexes ZnT(*n*-Pe)P and H_2T(*n*-Pe)P or the nominally planar tetraphenylporphyrins ZnTPP and H_2TPP. The ground-state ruffling distortions[9] exhibited by ZnT(*t*-Bu)P,[3a] and by analogy expected for H_2T(*t*-Bu)P, poise the macrocycle for

(1) (a) Washington University. (b) Present Address: Hunter College. (c) University of California. (d) Sandia National Laboratories. (e) University of New Mexico. (f) Present Address: Case Western Reserve University. (g) Brookhaven National Laboratory.

(2) (a) Ravikanth, M.; Chandashekar, T. K. *Struct. Bonding (Berlin)* **1995,** *82*, 105. (b) Deisenhofer, J.; Epp, O.; Sinning, I.; Michel, H. *J. Mol. Biol.* **1995**, *246*, 429. (c) Freer, A.; Prince, S.; Sauer, K.; Papaz, M.; Haithornthwaite-Lawless, A.; McDermott, G.; Cogdell, R.; Isaacs, N. W. *Structure* **1996**, *4*, 449. (d) Crane, B. R.; Siegl, L. M.; Getzoff, E. D. *Science* **1995**, *270*, 59. (e) Shelnutt, J. A.; Song, X. Z.; Ma, J.-G.; Jia, S.-L.; Jentzen, W.; Medforth, C. J. *Chem. Soc. Rev.* **1998**, *27*, 31.

(3) (a) Senge, M. O.; Ema, T.; Smith, K. M. *J. Chem. Soc., Chem. Commun.* **1995**, 733. (b) Barkigia, K. M.; Renner, M. W.; Furenlid, L. R.; Fajer, J. Unpublished.

(4) (a) Medforth, C. J.; Senge, M. O.; Smith, K. M.; Sparks, L. P.; Shelnutt, J. A. *J. Am. Chem. Soc.* **1992**, *114*, 9859. (b) Regev, A.; Galili, T.; Medforth, C. J.; Smith, K. M.; Barkigia, K. M.; Fajer, J.; Levanon, H. *J. Phys. Chem.* **1994**, *98*, 2520. (c) Nurco, D. J.; Medforth, C. J.; Forsyth, T. P.; Olmstead, M. M.; Smith, K. M. *J. Am. Chem. Soc.* **1996**, *118*, 10918. (d) Barkigia, K. M.; Nurco, D. J.; Renner, M. W.; Melamed, D.; Smith, K. M.; Fajer, J. *J. Phys. Chem. B* **1998**, *102*, 322. (e) Song, X.-Z.; Jaquinod, L.; Jentzen, W.; Nurco, D. J.; Jia, S.-L.; Khoury, R. G.; Ma, J.-G.; Medforth, C. J.; Smith, K. M.; Shelnutt, J. A. *Inorg. Chem.* In press.

(5) (a) Jentzen, W.; Simpson, M. C.; Hobbs, J. D.; Song, X.; Ema, T.; Nelson, N. Y.; Medforth, C. J.; Smith, K. M.; Veyrat, M.; Mazzanti, M.; Ramasseul, R.; Marchon, J.-C.; Takeuchi, T.; Goddard, W. A., III; Shelnutt, J. A. *J. Am. Chem. Soc.* **1995**, *117*, 11085. (b) Song, X.-Z.; Jentzen, W.; Jia, S.-L.; Jaquinod, L.; Nurco, D. J.; Medforth, C. J.; Smith, K. M.; Shelnutt, J. A. *J. Am. Chem. Soc.* **1996**, *118*, 12974. (c) Shelnutt, J. A.; Medforth, C. J.; Berber, M. D.; Barkigia, K. M.; Smith, K. M. *J. Am. Chem. Soc.* **1991**, *113*, 4077.

(6) (a) Gentemann, S.; Medforth, C. J.; Forsythe, T. P.; Nurco, D. J.; Smith, K. M.; Fajer, J.; Holten, D. *J. Am. Chem. Soc.* **1994**, *116*, 7363. (b) Gentemann, S.; Medforth, C. J.; Ema, T.; Nelson, N. Y.; Smith, K. M.; Fajer, J.; Holten, D. *Chem. Phys. Lett.* **1995**, *245*, 441. (c) Gentemann, S. G.; Nelson, N. Y.; Jaquinod, L. A.; Nurco, D. J.; Leung, S. H.; Smith, K. M.; Fajer, J.; Holten, D. *J. Phys. Chem. B* **1997**, *110*, 1247.

S0002-7863(97)04101-2 CCC: $15.00
Published on Web 04/07/1998

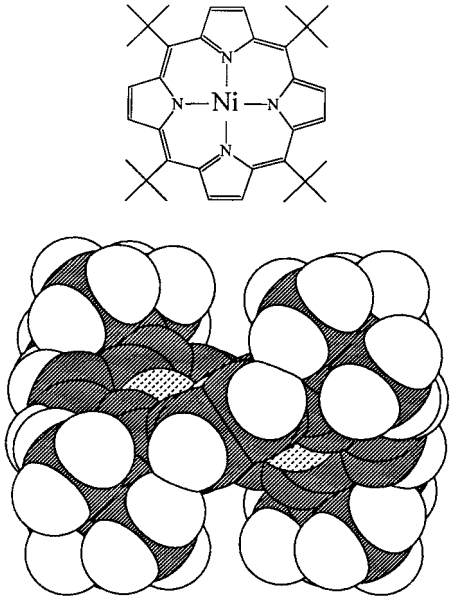

Figure 1. The NiT(*t*-Bu)P macrocycle (top) and a space-filling model based on the X-ray crystal structure of the molecule (bottom).[3b]

additional distortions in the $^1(\pi,\pi^*)$ excited state, which are evidenced by large shifts between the absorption and fluorescence maxima. These excited-state distortions in turn facilitate rapid nonradiative deactivation to the ground state, either directly or by concomitant modulation of the interactions between the porphyrin and the solvent. The photoinduced structural excursions of ZnT(*t*-Bu)P and H_2T(*t*-Bu)P are minimized at low temperature; at 77 K the excited-state lifetimes and fluorescence yields are similar to those of planar porphyrins, even though the molecules remain distorted in the ground state.[6b,c] This temperature behavior is unique among the nonplanar zinc and free base porphyrins studied to date.

We report here the results of extending these studies to the nickel(II) analogue, NiT(*t*-Bu)P (Figure 1), and the closely related tetraadamantyl complex, NiT(Ad)P. These molecules are highly distorted in solution, based on the X-ray data for NiT(*t*-Bu)P at 106 K that reveal a ruffled structure with a Ni−N distance of 1.869(7) Å,[3b] powder EXAFS data for NiT(*t*-Bu)P at 295 K that yield a Ni−N distance of 1.86(2) Å,[3b] analogy with the crystal structure of ZnT(*t*-Bu)P,[3a] Raman and optical spectra in solution,[5a] and molecular mechanics calculations (see ref 5a and below). A motivation for these studies is that a $(d_{z^2},d_{x^2-y^2})$ ligand-field excited state is a central intermediate in the deactivation of photoexcited low-spin d^8 nickel porphyrins, a process that involves the kinetic phases shown in Scheme 1.[8,10,11] Formation of the ligand-field excited state promotes changes in the structure of the porphyrin macrocycle, including a larger Ni−N distance to relieve the repulsion between the $d_{x^2-y^2}$ electron and those of the central nitrogens.[11] We anticipated that such conformational dynamics in the (d,d) excited state of NiT(*t*-Bu)P, in addition to those expected in the $^1(\pi,\pi^*)$ excited state, might lead to novel photophysical properties for this porphyrin. Indeed, we find an extraordinary dependence of the lifetime of the (d,d) excited state of NiT(*t*-Bu)P on both solvent dielectric properties and temperature, with the lifetimes spanning several picoseconds to several microseconds.

Scheme 1. Deactivation Pathway of Planar Low-Spin Nickel Porphyrins

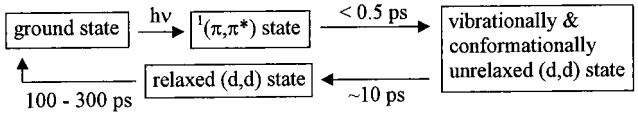

Materials and Methods

The NiT(*t*-Bu)P, NiT(Ad)P, NiT(*n*-Pe), and NiT(*i*-Pr)P complexes were prepared as described.[3a,5a] (The *meso* substitutents in these four complexes are respectively *tert*-butyl, adamantyl, *n*-pentyl, and isopropyl.) Solvents, generally HPLC grade, were used directly, distilled from an appropriate drying agent, or passed down an activated basic alumina column. Ultrafast transient absorption measurements were carried out as described elsewhere, and used 0.2-ps, 582-nm excitation flashes.[8] Lifetimes greater than 30 ns were measured with use of 30-ps, 532-nm excitation flashes and a detection scheme having an instrument response of 20 ns. In particular, the absorption changes were probed by using the filtered output of a CW xenon lamp that was passed through the sample and a monochromator and was detected by a Hamamatsu R928 photomultiplier tube whose output was read across a 93Ω terminator into a Tektronix 7912AD transient digitizer.

Transient Raman spectra were obtained by using 440-nm, 10-ns pulses from a Nd:YAG-pumped dye laser operating at 10 Hz. A cylindrical lens was used to loosely focus the incident beam at the sample. Incident fluxes at full laser power were estimated to be 10^4−10^5 W/cm^2. The intensity was attenuated as needed with neutral density filters. The signal was collected, telescoped to reduce the image at the slit, dispersed with a 0.5-m spectrograph, and detected with a liquid-N_2-cooled CCD array.

Classical molecular mechanics (MM) calculations were performed with POLYGRAF software (Molecular Simulations, Inc.) and a force field developed and modified by Shelnutt et al.[5b,12] The force field was formulated on the basis of normal-coordinate analyses of nickel porphyrins[13] and the DREIDING II force field.[14,15] Force constants

(7) (a) Rivikanth, M.; Reddy, D.; Chandrashekar, T. K. *J. Photochem. Photobiol. A: Chem.* **1993**, *72*, 61. (b) Charlesworth, P.; Truscott, T. G.; Kessel, D.; Medforth, C. J.; Smith, K. M. *J. Chem. Soc., Faraday Trans.* **1994**, *90*, 1073. (c) Kadish K. M.; Caelmebechel, E. V.; Boula, P.; D-Souza, F. D.; Vogel, E.; Kiskas, M.; Medforth, C. J.; Smith, K. M. *Inorg. Chem.* **1993**, *32*, 4177. (d) Tsuchiya, S. *Chem. Phys. Lett.*, **1990**, *169*, 608. (e) Takeda, J.; Sato, M. *Chem. Lett.* **1995**, 939. (f) Lin, C.-Y.; Hu, S.; Rush, T. III; Spiro, T. G. *J. Am. Chem. Soc.* **1996**, *118*, 9452.

(8) Drain, C. M.; Kirmaier, C.; Medforth, C. J.; Nurco, D. J.; Smith, K. M.; Holten, D. *J. Phys. Chem.* **1996**, *100*, 11984−11993.

(9) The ruffle distortion is characterized by clockwise and counterclockwise twisting of alternating pyrrole rings, with alternate meso carbons lying above and below the mean macrocycle plane. The saddle distortion is characterized by alternate up and down tilting of pyrrole rings with respect to the mean plane, and the four *meso* carbons lying in that plane (Scheidt, W. R.; Lee, Y. J.. *Struct. Bonding (Berlin)* **1987**, *64*, 1).

(10) (a) Kobayashi, T.; Straub, K. D.; Rentzepis, P. M. *Photochem. Photobiol.* **1979**, *29*, 925. (b) Chirvonyi, V. S.; Dzhagarov, B. M.; Timinskii, Y. V.; Gurinovich, G. P. *Chem. Phys. Lett.* **1980**, *70*, 79. (c) Kim, D.; Kirmaier, C.; Holten, D. *Chem. Phys.*, **1983**, *75*, *305*. (d) Rodriguez, J.; Holten, D. *J. Chem. Phys.* **1989**, *91*, 3525. (e) Rodriguez, J.; Holten, D. *J. Chem. Phys.* **1990**, *92*, 5944. (f) Eom, H. S.; Jeoung, S. C.; Kim, D.; Ha, J.-H.; Kim, Y-.R. *J. Phys. Chem. A.* **1997**, *101*, 3661.

(11) (a) Findsen, E. W.; Shelnutt, J. A.; Ondrias, M. R. *J. Phys. Chem.* **1988**, *92*, 307. (b) Courtney, S. H.; Jedju, T. M.; Friedman, J. M.; Alden, R. G.; Ondrias, M. R. *Chem. Phys. Lett* **1989**, *164*, 39. (c) Sato, S.; Kitigawa, T. *Appl. Phys.* **1994**, *B59*, 415. (d) Kruglik, S. G.; Mizutani, Y.; Kitigawa, T. *Chem. Phys. Lett.* **1997**, *266*, 283.

(12) (a) Shelnutt, J. A.; Majumder, S. A.; Sparks, L. D.; Hobbs, J. D.; Medforth, C. J.; Senge, M. O.; Smith, K. M.; Miura, M.; Quirke, J. M. E. *J. Raman Spectrosc.* **1992,** *23*, 523. (b) Song, X.; Jentzen, W.; Jaquinod, L.; Khoury, R. G.; Medforth, C. J.; Jia, S.; Ma, J.; Smith, K. M.; Shelnutt, J. A. *Inorg. Chem.* In press.

(13) (a) Li, X.-Y.; Czernuzewics, R. S.; Kincaid, P.; Spiro, T. G. *J. Am. Chem. Soc.* **1989**, *111*, 7012. (b) Li, X.-Y.; Czernuzewics, R. S.; Kincaid, J. R.; Su, Y. O.; Spiro, T. G. *J. Phys. Chem.* **1990**, *94*, 31. (c) Li, X.-Y.; Czernuzewics, R. S.; Kincaid, J. R.; Stein, P.; Spiro, T. G. *J. Phys. Chem.* **1990**, *94*, 47.

(14) Sparks, L. D.; Medforth, C. J.; Park, M.-S.; Chamberlain, J. R.; Ondrias, M. R.; Senge, M. O.; Smith, K. M.; Shelnutt, J. A. *J. Am. Chem. Soc.* **1993**, *115*, 581.

(15) Mayo, S. L.; Olafson, B. D.; Goddard, W. A., III. *J. Phys. Chem.* **1990**, *94*, 88.

for the bond stretches, bond angle bends, bond torsions, and inversions of the porphyrin macrocycle were initially taken from the normal coordinate analysis of NiOEP. The most significant modification to the initial force field is that the out-of-plane force constants of Li *et al.*[13a] were reduced by 50% because of theoretical considerations such that a group of nonplanar porphyrin reference structures were accurately calculated.[5b] For nickel in the $(d_{z^2},d_{x^2-y^2})$ configuration, the Ni−N equilibrium bond length was set to 2.07 Å, a value obtained by modeling the structures of high-spin six-coordinate nickel porphyrins. The van der Waals parameter for $(d_{z^2},d_{x^2-y^2})$ nickel was taken to be the same as for zinc, and obtained from the DREIDING II force field.[15] The transition barriers between different conformers were determined by minimizing the structure with the $C_\beta C_\alpha - C_m C_s$ dihedral angle systematically constrained at different values until the peripheral substituent moved through the porphyrin mean plane and the porphyrin conformation changed.[16] The barrier energy was estimated from the energy of the constrained structure obtained just before interconversion.

Semiempirical quantum calculations were performed by using the INDO/restricted Hartree−Fock method developed and optimized for spectroscopic predictions by Zerner and co-workers.[17] HyperChem (Hypercube, Inc.) software was used, with the β(d) parameter set to 32. Molecular structures were obtained from the classical energy-optimization calculations. The calculations were performed on the entire molecular structure, including the substituents. The configuration-interaction calculations included single excitations from the 25 top-filled orbitals to the 10 lowest-empty orbitals, including both the d_{z^2} and $d_{x^2-y^2}$ metal orbitals. The orbital populations were restricted to calculate the lowest-energy singlet state of the porphyrin.

Results

Studies of NiT(*t*-Bu)P as a Function of the Dielectric Properties of Noncoordinating Solvents at 295 K. Representative transient absorption difference spectra for NiT(*t*-Bu)P in toluene at room temperature are shown in Figure 2, panels A and B. The spectrum observed at 0.5 ps forms with the 0.2-ps excitation flash and is dominated by bleaching of the ground-state Soret band. This spectrum is assigned to the $^1(\pi,\pi^*)$ excited state of the macrocycle. These early-time absorption changes decay with a time constant of 0.8 ± 0.2 ps to a spectrum having an asymmetric derivative-like shape (5.5-ps spectrum in Figure 2A). This spectrum continues to evolve with complex wavelength-dependent kinetics. The average time constant of the second kinetic phase measured between 425 and 475 nm is 7 ps, but values ranging from 2 to 20 ps are observed as a function of wavelength. The resultant spectrum (40-ps spectrum) has a symmetric derivative-like shape composed of the bleaching of the ground-state Soret band overlapped with an opposing excited-state Soret absorption to the blue. The presence of both the 0.8-ps decay of the $^1(\pi,\pi^*)$ state and the subsequent 7-ps component is readily seen from the kinetic trace at 465 nm, where the two kinetic phases have opposite signs for the change in ΔA with time (Figure 2A inset). In analogy with previous results on other nickel porphyrins, the derivative-shaped spectra are assigned to the metal (d,d) excited state, and the complex 7-ps spectral evolution is ascribed to vibrational relaxation and conformational readjustments within this state.[8,10,11]

The (d,d) excited state undergoes only a modest decay between 40 ps and 2.7 ns (Figure 2B). Kinetic data on a longer time scale obtained using a 30-ps excitation flash reveal that both the excited-state absorption (450 nm) and ground-state bleaching (470 nm) decay with a time constant of 29 ± 3 ns

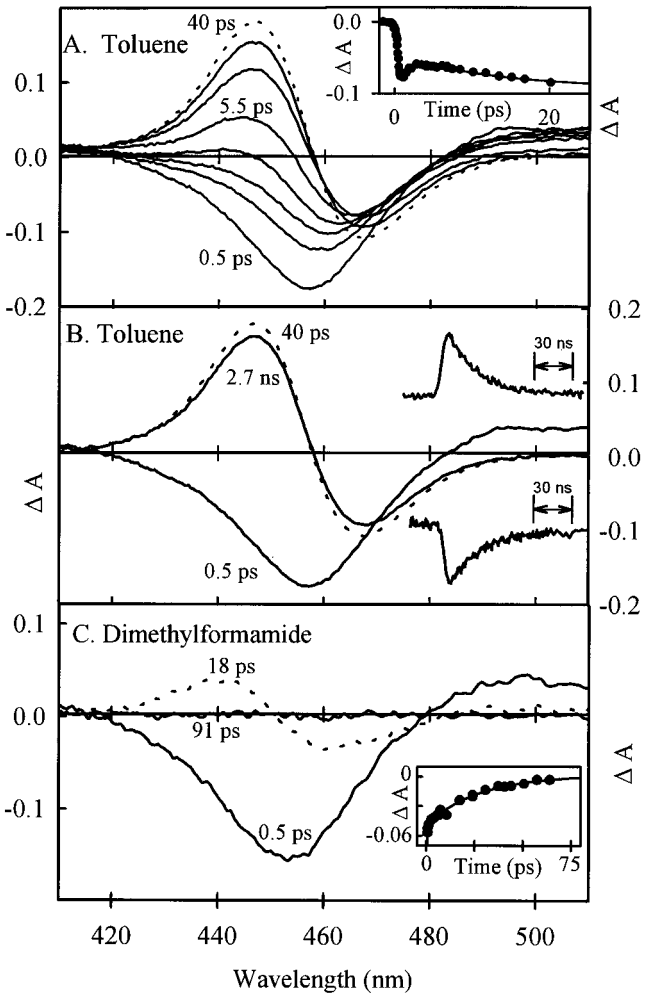

Figure 2. Transient absorbance difference spectra ($A_{excited} - A_{unexcited}$) for NiT(*t*-Bu)P at room temperature in toluene (A and B) and dimethylformamide (C), acquired using 0.2-ps, 582-nm excitation flashes. The spectra in panel A were acquired at 0.5, 1.8, 2.1, 3.5, 5.5, 11, 20, and 40 ps after excitation. The inset to panel A is a kinetic trace and fit at ~470 nm showing the instrument response (initial downward deflection) followed by two kinetic components having time constants of 0.8 and 7 ps. The kinetic traces in panel B span ~100 ns and were obtained by using 30-ps excitation flashes. The traces show the decay of the transient absorption at 450 nm and of the ground-state bleaching at 470 nm; both have a time constant of 29 ns. The kinetic data and fit in inset to panel C were obtained at 470 nm and have a time constant of 22 ps.

(Figure 2B insets). During this time, an isosbestic point is found at 457 nm and $\Delta A = 0$ (see 40-ps and 2.7-ns spectra in Figure 2B). Collectively, these findings are consistent with simultaneous deactivation of the (d,d) excited state and complete electronic and structural recovery of the ground state with a time constant of 29 ns for NiT(*t*-Bu)P in toluene at 295 K.

In nearly all of the other 34 solvents in which NiT(*t*-Bu)P was studied, the same basic behavior is observed at early times after photoexcitation. Namely, there is a 0.5−1 ps component ascribed to decay of the $^1(\pi,\pi^*)$ state and formation of the ligand-field excited state, and a kinetically complex second phase with an average time constant of 5−10 ps ascribed to vibrational/conformational relaxation within the (d,d) excited state. However, the subsequent decay of the (d,d) excited state to the ground state shows a substantial solvent dependence. These findings are illustrated in Figure 2C by the data for NiT(*t*-Bu)P in dimethylformamide (DMF). The $^1(\pi,\pi^*)$ spectrum at 0.5 ps is basically identical to that observed in toluene (see

(16) Jia, S.-L.; Zhang, J.; Ma, J.-G.; Shelnutt, J. A. In preparation.
(17) (a) Ridley, J. E.; Zerner, M. C. *Theor. Chim. Acta* **1973**, *32*, 111. (b) Bacon, A.; Zerner, M. C. *Theor. Chim. Acta* **1979**, *53*, 21. (c) Zerner, M. C.; Loew, G. H.; Kirchner, R. F.; Mueller-Westerhoff, U. T. *J. Am. Chem. Soc.* **1980**, *102*, 589. (d) Edwards, W. D.; Weiner, B.; Zerner, M. C. *J. Phys. Chem.* **1988**, *92*, 6188.

Table 1. Solvent Dependence of (d,d) Lifetime of NiT(*t*-Bu)P at 295 K[a]

solvent	τ(d,d)	ϵ	d	ET30	$\lambda = (1/n^2) - (1/\epsilon)$	(π,π^*)/(d,d)
A. nonligating or potentially weakly ligating solvents (squares in Figure 3)						
benzene (wet or dry)	46 ns	2.3	0	34.3	0.01	0.77
toluene	29 ns	2.4	0.4	33.9	0.03	0.77
methylcyclohexane	32 ns	2	0	(31)	−0.01	0.67
cyclohexane	31 ns	2	0	30.9	−0.01	0.71
mineral oil	30 ns	(2)	0.2	(31)	(0.01)	1
2,2,5,5-Me_4-THF	1.3 ns	(6)		(35)	(0.34)	0.83
o-dichlorobenzene	0.56 ns	9.9	2.5	38	0.31	1.1
2,6-dimethylpyridine	0.54 ns	7.3	1.7	36.9	0.31	0.83
2,2,6,6-tetramethylpiperidine	0.54 ns	(3)		(32)	(0.14)	0.77
chlorobenzene	0.38 ns	5.6	1.7	36.8	0.25	1.4
quinoline	0.32 ns	9	2.3	39.4	0.27	0.83
nitrobenzene	0.11 ns	34.8	4.2	41.2	0.38	1.4
2-nitrotoluene	0.11 ns	27.4	4.1	(41)	0.38	1.4
benzonitrile	82 ps	25.2	4.2	41.5	0.39	2
dimethylformamide	22 ps	36.7	3.8	43.8	0.44	2.5
dimethyl sulfoxide	18 ps	48.9	4.0	45.1	0.44	5
nitromethane	2 ps	38.6	3.5	46.3	0.5	5
B. potentially more strongly ligating solvents (circles in Figure 3)						
nitrogenous						
2-methylpyridine	0.l4 ns	9.8	1.5	38.3	0.35	1.1
2,5-dimethylpyrrolidine	0.10 ns	(9)		(36)	(0.37)	1.1
piperidine	75 ps	5.8	1.2	35.5	0.3	1.43
aniline	54 ps	6.9	1.8	44.3	0.25	3.3
pyridine	28 ps	12.3	2.2	40.5	0.36	1.7
pyrrolidine	26 ps	(6)	1.6	39.1	(0.31)	3.3
oxygenous						
2,5-dimethyltetrahydrofuran	0.13 ns	(6)		35.5	(0.34)	0.8
methyl(*tert*-butyl)ether	0.11 ns	(4)	1.2	35.5	(0.28)	0.91
anisole	0.10 ns	4.3	1.3	37.1	0.2	1
3-pentanone	74 ps	17	2.7	39.3	0.52	1.4
2-methyltetrahydrofuran	51 ps	7		36.5	(0.37)	
cyclohexanone	41 ps	18.3	2.9	39.8	0.42	2
tetrahydrofuran (THF)	26 ps	7.4	1.8	37.4	0.37	1.7
diethyl ether	24 ps	4.3	1.2	34.5	0.31	2
1,4-dioxane	10 ps	2.2	0	36	0.04	5

[a] The lifetimes were measured at 295 K and have errors of ±10%. The solvent parameters[18] are the dielectric constant (ϵ), dipole moment (d), ET30, Marcus reorganization parameter (λ), and refractive index (n). The values in parentheses were estimated from comparison with data for related solvents.

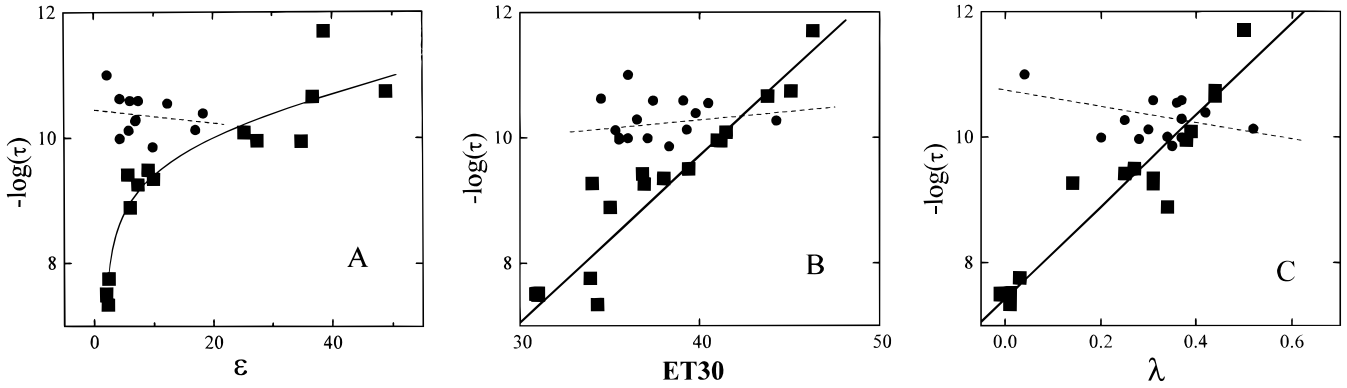

Figure 3. Dependence of the (logarithm of the) lifetime of the (d,d) excited state of NiT(*t*-Bu) on three measures of solvent dielectric properties: (A) dielectric constant (ϵ), (B) the ET30 empirical solvent parameter, and (C) the Marcus solvent reorganization parameter $\lambda = (1/n^2) - (1/\epsilon)$, where n is the refractive index. The data depicted by the squares are for the solvents in list A in Table 1 while those depicted by circles are from list B. The lines are shown only to clarify the trends in the data.

Figure 2B), except for a small shift in the position of the Soret bleaching that parallels the Soret maximum in the ground-state spectrum. The spectrum at 18 ps is assigned to the (d,d) excited state and has the same derivative shape as the (d,d) spectrum in toluene (40-ps spectrum in Figure 2B), but with a reduced amplitude (relative to the initial Soret bleaching near 450 nm) and a blue shift of the $\Delta A = 0$ point. The most notable difference from the behavior in toluene is that the excited-state absorption and ground-state bleaching in DMF decay with a time constant of only 22 ± 3 ps (Figure 2C inset). This (d,d) lifetime is 1300 times shorter than that found in toluene!

Excited-state lifetimes for NiT(*t*-Bu)P in a number of noncoordinating solvents (and several potentially weakly coordinating solvents) are given in Table 1, list A. These data are plotted in Figure 3 (squares and solid lines). This figure shows the remarkable dependence of the (d,d) lifetime of NiT(*t*-Bu)P on three measures of the dielectric properties of the solvent: The first parameter (Figure 3A) is the static dielectric

constant (ϵ). The second variable (Figure 3B) is the ET30 empirical solvent parameter, which like ϵ primarily reflects solvent polarity. ET30 also incorporates other solvation factors (such as polarizability) that affect the position of the charge-transfer absorption band of a beteine dye.[18a] The third parameter (Figure 3C) is the Marcus solvent reorganization parameter $\lambda = [(1/n^2) - (1/\epsilon)]$, which is a function of the static dielectric constant (polarity) and the high-frequency dielectric constant (the square of the refractive index (n) reflecting polarizability).[19] Table 1 also shows that the lifetime depends similarly on dipole moment. The lifetime decreases by a factor greater than 10^4 from 46 ns in the nonpolar benzene to 2 ps in the very polar nitromethane. It is noteworthy that, in each solvent, the decay of the (d,d) excited state is accompanied by isosbestic points (see, e.g., Figure S1 of the Supporting Information) and is well described by single-exponential kinetics. This behavior is consistent with the decay of a single excited state in each solvent. It is not consistent with the parallel decay of two states or forms, one with a short lifetime (picoseconds) and the other with a long lifetime (nanoseconds), whose relative contributions vary with solvent properties.

That the variations in excited-state lifetime shown in Figure 3 (squares and solid lines) are due primarily to solvent dielectric properties is supported further by analysis of other possible solvent effects. First, the effect of viscosity on the (d,d) lifetime of NiT(*t*-Bu)P is very small considering that the viscosity (η) of nitromethane ($\eta = 0.62$ Cp, $\tau = 2$ ps) is comparable to that of benzene ($\eta = 0.61$ Cp, $\tau = 46$ ns), and that the lifetime in benzene (and in other hydrocarbons) is similar to that in the highly viscous medium mineral oil ($\eta = 110$ Cp, $\tau = 30$ ns). Second, a possible role of adventitious water in the more polar solvents (even though they were dried) is eliminated by the observation that the same lifetime (46 ns) is obtained in both dry and water-saturated benzene. Third, metal coordination or porphyrin−solvent redox reactions cannot explain the substantial variation in lifetime that occurs among a majority, if not all, of the solvents in list A of Table 1 (Figure 3, squares). If electron transfer from the photoexcited nickel porphyrin to a solvent were important, one would have expected the effect to be more significant for nitrobenzene than for nitromethane, which is contrary to what is observed. Additionally, the solvents under discussion are either noncoordinating or at most weakly coordinating to nickel porphyrins. These considerations for the solvents in list A argue that solvent polarity, perhaps in conjunction with polarizability, is primarily responsible for the variation of the lifetime of the (d,d) excited state of NiT(*t*-Bu)P.

Additional Solvent Effects on the Photodynamics of NiT(*t*-Bu)P at 295 K. In some solvents, factors *in addition to* dielectric properties come into play in modulating the (d,d) lifetime of NiT(*t*-Bu)P. These solvents are included in list B of Table 1, and the lifetimes are plotted in Figure 3 as circles. The (d,d) lifetime of NiT(*t*-Bu)P in these solvents ranges from 10 to 140 ps. These values are generally shorter than those found in the solvents in list A that have similar dielectric properties. The solvents in list B include nitrogenous bases such as pyridine and piperidine that are known to coordinate to the metal in other nickel porphyrins such as NiTPP to form high-spin six-coordinate complexes.[10c,e,20] However, the behavior of NiT(*t*-Bu)P in these heteroatom-containing solvents is unlike that normally expected for metal coordination to nickel porphyrins. (i) The ground-state Soret position varies by only about 5 nm among the 34 solvents used in this study, including the nitrogenous bases. This behavior is unlike the significant effect of metal ligation on the spectra of other nickel porphyrins. (ii) Ground-state recovery is complete within 150 ps after excitation of NiT(*t*-Bu)P in potentially ligating solvents (e.g., piperidine). This behavior is contrary to the long (>10 ns) lifetimes found previously either upon ligand release from photoexcited six-coordinate nickel porphyrins or upon ligand binding to photoexcited four-coordinate nickel porphyrins in the presence of potential ligands.[10c,e,f] (iii) Deactivation is more rapid in pyridine than in piperidine even though the latter is the stronger σ-donor. This finding is not consistent with a metal-coordination effect, but is in keeping with the greater polarity of pyridine than piperidine. (iv) The lifetimes in the oxygen-containing solvents in list B are comparable to those found in the nitrogenous bases (Table 1). This behavior is contrary to what would be expected for axial ligation given that oxygen-containing ligands are generally weaker σ-donors than the nitrogenous bases and coordinate only weakly to nickel porphyrins. In agreement with these last two points, the lifetimes for the solvents in either list A or B do not track the electron-donating ability of the solvents as reflected by parameters such as the donor number.

Thus, the spectral and kinetic results for NiT(*t*-Bu)P in heteroatom-containing solvents do not coincide with the behavior *normally* expected for axial ligation to nickel porphyrins, in either the ground or excited electronic state. Nonetheless, some of the solvents in list B do appear to interact with the metal or the macrocycle in NiT(*t*-Bu)P, resulting in shorter lifetimes than observed in the solvents in list A with similar dielectric properties: there appears to be a correlation between steric bulk adjacent to the heteroatom of the solvent and the excited-state lifetime. The more bulky solvents induce lifetimes that approach values expected solely on dielectric properties (Table 1 and Figure 3). For example, the lifetimes in 2,2,5,5-tetramethyltetrahydrofuran (1.3 ns) and 2,6-dimethylpyridine (0.54 ns) fall near or on the dielectric-properties lines in Figure 3 (solid), whereas the analogues with progressively fewer methyl groups exhibit shorter lifetimes terminating in values of 26 ps for tetrahydrofuran and 28 ps for pyridine. Note that if the solvents in list B (and perhaps a few in list A) do form ground- or excited-state adducts with NiT(*t*-Bu)P, the consequence is to make the excited-state deactivation rates more "normal", i.e., comparable to the 100−300 ps found for less distorted or nominally planar complexes such as NiT(*n*-Pe)P and NiTPP in noncoordinating solvents (see Table 1 and below). These considerations further illustrate the unusual dependence of the photodynamics of NiT(*t*-Bu)P on solvent properties.

Temperature Dependence of the Photodynamics of NiT(*t*-Bu)P. The effects of temperature on the lifetime of the (d,d) excited state of NiT(*t*-Bu)P are shown in Table 2 and Figure 4. The lifetime in 2-methyltetrahydrofuran increases from 51 ps at 295 K to 5.8 μs at 85 K (squares). Since the lifetime changes smoothly through the ~150 K freezing point of this solvent, the temperature dependence of the lifetime cannot be ascribed to a phase transition in the medium. A similar temperature dependence is found in DMF, as deduced from several measurements above the freezing point of the solvent. An activation enthalpy of ~3 kcal/mol is estimated from the Arrhenius plot of the (d,d) lifetime in the two solvents (Figure 4, solid line). A somewhat smaller activation energy of ~1 kcal/mol is estimated for the (d,d) decay process in several nonpolar solvents

(18) (a) Reichardt, C. *Solvent Effects in Organic Chemistry*; VCH Publishers: Meinheim, 1988. (b) *Handbook of Chemistry and Physics*, 78th ed.; Lide, David, R., Ed.; CRC Press: New York, 1991. (c) Gordon, A. J.; Ford, R. A. *The Chemists Companion*; John Wiley & Sons: New York, 1972. (d) McClellan, A. L. *Tables of Experimental Dipole Moments*; W. H. Freeman and Co.: San Francisco, 1963.

(19) Marcus, R. A.; Sutin, N. *Biochim. Biophys. Acta*, **1985**, *811*, 265.

Table 2. Temperature Dependence of (d,d) Lifetime of NiT(*t*-Bu)P[a]

solvent	temp (K)	τ(d,d)
toluene	295	29 ns
	250	58 ns
	225	93 ns
	190	0.12 μs
	180	0.11 μs
	170	0.15 μs
	160	0.16 μs
3-methylpentane	295	35 ns
	240	70ns
	200	0.13 μs
	175	0.19 μs
	150	0.30 μs
	135	0.34 μs
	110	1.6 μs
	80	2.5 μs
methylcyclohexane	295	32 ns
	210	0.15 μs
	170	0.28 μs
	150	0.34 μs
methylcyclopentane	295	50 ns
	180	0.26 μs
	140	0.35 μs
dimethylformamide	295	22 ps
	245	91 ps
	225	0.14 ns
	220	0.33 ns
2-methyltetrahydrofuran	295	51 ps
	220	0.29 ns
	180	0.77 ns
	160	2.8 ns
	130	0.11 μs
	110	0.38 μs
	100	1.1 μs
	85	5.8 μs

[a] Lifetimes have errors of ±10%.

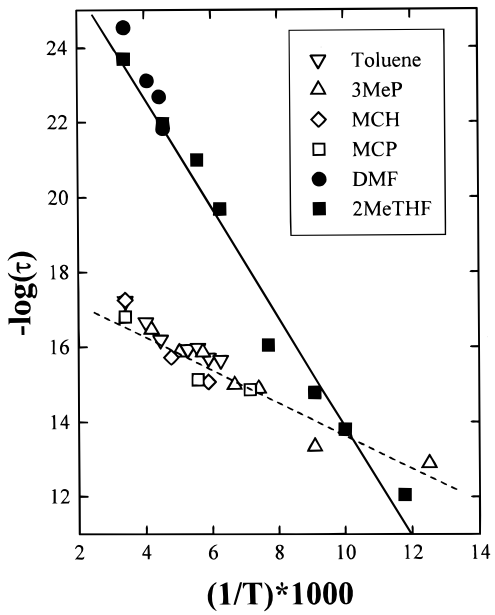

Figure 4. Arrhenius plots of the (d,d) lifetime of NiT(*t*-Bu)P in various solvents. The polar solvents (closed symbols) are dimethylformamide and 2-methytetrahydrofuran. The nonpolar solvents (open symbols) are toluene, 3-methylpentane, methylcyclohexane, and methylcyclopentane. The lines are fits that yield activation enthalpies of ~3 kcal/mol (solid, polar solvents) and ~1 kcal/mol (dashed, nonpolar solvents).

(Figure 4, dashed line). These solvents include 3-methylpentane, for which the (d,d) lifetime varies reasonably smoothly from about 40 ns at 295 K, through the 119 K freezing point of the solvent, to 2.5 μs at 80 K. (The entropy factors derived from the intercepts of the Arrhenius plots are also somewhat larger for the polar versus nonpolar media.) Collectively, these data show that although the lifetimes of the ligand-field excited state of NiT(*t*-Bu)P in nonpolar and highly polar solvents differ by over 3 orders of magnitude at room temperature, the lifetimes in both types of solvent lengthen and converge to several microseconds near 80 K.

Environmental Effects on the Transient Optical Spectrum of NiT(*t*-Bu)P. The factors responsible for the variation in the (d,d) lifetime of NiT(*t*-Bu)P with solvent dielectric properties and temperature also influence the excited-state absorption difference spectrum (see Figure 2). Less polar solvents and lower temperatures give rise to longer lifetimes accompanied by larger amplitudes of the Soret-region (d,d) spectrum (peak to trough $\Delta\Delta A$ in the derivative-shaped spectrum) relative to the peak amplitude of the Soret bleaching in the $^1(\pi,\pi^*)$ spectrum. (This ratio normalizes the amplitude of the (d,d) spectrum to the same initial concentration of photoexcited molecules.) For example, the maximum relative amplitude of the (d,d) spectrum in DMF (18-ps spectrum relative to the 0.5-ps spectrum in panel C of Figure 2) is about 30% of that in toluene (40-ps spectrum relative to the 0.5-ps spectrum in panel A). The behavior in other solvents is given in Table 1 and Figure S2 of the Supporting Information.

Spectra were also acquired for NiT(*t*-Bu)P in selected solvents at room temperature in the Q-band region (500−650 nm), where the (π,π^*) absorption is relatively featureless (data not shown). These data *do not* show appreciable decay of the ground-state Q-band bleachings during either the $^1(\pi,\pi^*)$ lifetime ($\tau = 0.5-1$ ps) or the time for vibrational/conformational relaxation within the (d,d) state ($\tau = 5-10$ ps) and, most importantly, the behavior does not depend significantly on solvent. Hence, the reduced amplitude of the Soret-region (d,d) spectra observed in polar versus nonpolar solvents (or high versus low temperatures) does not reflect significantly enhanced deactivation of $^1(\pi,\pi^*)$ to the ground state, but rather must be due largely to environmental effects on the relative positions of the ground- and excited-state Soret bands (and thus to different degrees of cancellation of these features in the transient difference spectra).

Excited-State Lifetimes for Other Nickel Porphyrins. Preliminary data on nickel tetraadamantylporphyrin (NiT(Ad)P) indicate that the (d,d) excited state lifetime obeys a similarly strong dependence on solvent dielectric properties (Table 3). In each solvent examined to date, the (d,d) lifetime is somewhat longer for NiT(Ad)P than for NiT(*t*-Bu)P: 40 ns versus 29 ns in toluene, 0.54 ns versus 0.34 ns in chlorobenzene, 65 ps versus 28 ps in pyridine. It is likely that the bulkier substituents of NiT(Ad)P induce a still more distorted ground-state structure than that of NiT(*t*-Bu)P.[5a] Consequently, the excited-state conformational landscape of NiT(Ad)P may be reasonably expected to differ even more from planar analogues than that of NiT(*t*-Bu)P, leading to still slower deactivation to the ground state.

In contrast with NiT(*t*-Bu)P and NiT(Ad)P, the excited-state deactivation rates of less distorted or nominally planar nickel porphyrins[5a] such as NiT(n-Pe)P and NiTPP are much different than those found for the highly ruffled complexes (Table 3). For example, the (d,d) lifetimes of 100−220 ps for NiT(*n*-Pe)P, NiT(*i*-Pr)P, and NiTPP in toluene are *orders of magnitude shorter* than the values of 33 and 40 ns found for NiT(*t*-Bu)P and NiT(Ad)P in this solvent. Furthermore, the excited-state lifetimes of NiT(*n*-Pe)P and NiTPP do *not* change significantly in solvents with different dielectric properties and in which the

Table 3. Lifetimes of Other Nickel Porphyrins[a]

compound/solvent	(d,d) lifetime
NiT(Ad)P	
toluene	40 ns
mineral oil	40 ns
chlorobenzene	0.54 ns
2-nitrotoluene	0.22 ns
pyridine	65 ps
NiT(*n*-Pe)P	
toluene	94 ps
chlorobenzene	0.10 ns
dimethylformamide	0.12 ns
3-methylpentane	0.22 ns
NiT(*i*-Pr)P	
toluene	0.10 ns
NiTPP	
toluene	0.22 ns[b]
toluene at 200 K	0.22 ns
toluene at 170 K	0.30 ns
toluene/acetone 60/40	0.26 ns
toluene/acetone 60/40 at 170 K	0.31 ns
2-nitrotoluene	0.25 ns
chlorobenzene	0.20 ns
NiDPP	
toluene	0.12 ns[c]
methylcyclohexane	0.14 ns[c]
chlorobenzene	50 ps
dimethylformamide	45 ps

[a] Lifetimes (±10%) at 295 K unless noted otherwise. [b] Similar values are reported in ref 10. [c] From ref 8.

decay time for NiT(*t*-Bu)P varies by 3 orders of magnitude (Tables 1 and 3). This is true in the highly polar solvent DMF despite the fact that neither NiT(*n*-Pe)P, nor NiTPP, nor NiT(*t*-Bu)P show evidence of solvent coordination to the metal either before or after photoexcitation. Similarly, the (d,d) lifetime of NiTPP is only moderately sensitive to temperature, whereas the decay of photoexcited NiT(*t*-BuP) varies by orders of magnitude under similar conditions (Tables 2 and 3).

Table 3 also includes some representative data for nickel 2,3,5,7,8,10,12,13,15,17,18,20-dodecaphenylporphyrin (NiDPP). Data for this complex and related dodecaarylporphyrins suggest that NiDPP in solution can access multiple nonplanar conformations involving varying degrees of mixing of ruffle and saddle distortions in both the ground and excited electronic states.[4,8] The 120-ps (d,d) lifetime of NiDPP in toluene at 295 K falls in the range of values found for less distorted or nominally planar complexes such as NiT(*n*-Pe)P and NiTPP, but is significantly shorter than the 33-ns lifetime of the highly ruffled NiT(*t*-Bu)P under these conditions. Furthermore, the lifetime for NiDPP decreases by only a factor of about 3 to 45 ps in DMF, whereas the lifetime of NiT(*t*-Bu)P decreases by a factor of 1300 in this solvent.[21] Collectively, these comparisons indicate that the excited-state behaviors of NiT(*t*-Bu)P and NiT(Ad)P are not only significantly different from nominally planar porphyrins, but may also be unique among nonplanar nickel porphyrins.

Transient Raman Measurements. The photodynamic behavior of NiT(*t*-Bu)P was also probed by transient resonance Raman spectroscopy. At low incident laser fluxes, the spectrum for NiT(*t*-Bu)P in toluene is dominated by Raman scattering from the ground electronic state. The positions of structure-sensitive skeletal vibrations such as ν_4 (1358 cm^{-1}) and ν_2 (1536 cm^{-1}) match those obtained from CW resonance Raman spectroscopy.[15a] These positions are expected for a highly nonplanar porphyrin such as NiT(*t*-Bu)P and occur at much lower frequencies than observed for planar analogues such as NiTPP. At increasingly higher laser fluxes, the population of the (d,d) excited state builds up progressively more during the 10-ns laser pulse, and Raman scattering from this excited state contributes increasingly more to the observed spectrum. The Raman bands for the ligand-field excited state occur at significantly lower frequencies ($\nu_4 \sim 1342$ cm^{-1}, $\nu_2 \sim 1530$ cm^{-1}) than for the ground state, and the bands are broader by a factor of 2 to 3. The finding that the structure-sensitive ν_4 and ν_2 modes occur at lower frequencies for the (d,d) state versus the ground state is consistent with an expansion of the porphyrin core in the photoexcited complex, as has been observed for other nickel porphyrins.[10f,11] However, the excited-state shifts for NiT(*t*-Bu)P are slightly larger (~15 cm^{-1} for ν_4) than is generally observed for more planar porphyrins such as nickel protoporphyrin(IX) dimethyl ester (NiPPDME). In the 300 to 650 cm^{-1} region of the Raman spectrum of NiT(*t*-Bu)P, only intensity differences are found for the ground state versus the (d,d) excited state.

Similar behavior is observed for NiT(*t*-Bu)P in pyridine. The peak positions of the ν_4 and ν_2 modes for the ligand-field excited state (1340 and 1527 cm^{-1}) occur at significantly lower frequencies than for the ground state (1355 and 1534 cm^{-1}). The similarity of the Raman spectral characteristics of NiT(*t*-Bu)P in toluene and pyridine strongly supports the conclusion reached from the optical data that potentially coordinating solvents such as pyridine in fact do not ligate to the metal in either the ground state or the ligand-field excited state of NiT(*t*-Bu)P. In keeping with the shorter (d,d) lifetime of NiT(*t*-Bu)P in pyridine (28 ps) versus toluene (29 ns), significantly higher laser fluxes are required in pyridine than in toluene to obtain Raman signals of comparable magnitude in the two solvents.

Finally, previous studies of NiPPDME have revealed a solvent-polarity dependence of the frequencies of other Raman bands (e.g., ν_3 and ν_{10}) for the (d,d) state but not for the ground state.[11a] One would expect a similar effect for NiT(*t*-Bu)P, especially considering the observed dependence of the (d,d) lifetime of this molecule on solvent dielectric properties (Figure 2). However, these bands are not resolved for this highly nonplanar *meso*-substituted porphyrin. Nonetheless, the collective transient Raman data strongly support the results and conclusions from the time-resolved absorption studies concerning the effects of solvent on the spectral and kinetic properties of the ligand-field excited state of NiT(*t*-Bu)P. A full description of the transient Raman studies of NiT(*t*-Bu)P will be reported elsewhere.[22]

Molecular Mechanics and INDO Calculations. Classical molecular mechanics (MM) calculations were performed to gain insight into the most likely low-energy molecular conformations of NiT(*t*-Bu)P, for both the ground electronic state and the ligand-field excited state. For the ground state, the central nickel has a $(d_{z^2})^2$ configuration, and the equilibrium Ni−N distance in the MM calculations was set to 1.855 Å.[5a,c] For the ligand-field excited state, the central nickel has a $(d_{z^2},d_{x^2-y^2})$ configuration, and the equilibrium Ni−N distance was set to 2.070 Å,

(20) (a) McLees, B. D.; Caughey, W. S. *Biochemistry* **1968**, *7*, 642. (b) Lamar, G. N.; Walker, F. A. In *The Porphyrins*; Dolphin, D., Ed.; Academic Press: New York; 1978; Vol. IV, p 4.

(21) Unlike NiT(*t*-Bu)P, the (d,d) lifetime of NiDPP slows significantly as the viscosity of the medium is increased (Table 3), and this effect has been ascribed to requisite movement of the phenyl rings accompanying excited-state deactivation.[8] This viscosity effect must also contribute significantly to the lengthening of the (d,d) lifetime of NiDPP at low temperature.[8] Thus, the combined data suggest that the temperature dependence of the deactivation time of NiDPP originates from different factors than those operative for NiT(*t*-Bu)P.

(22) Simpson, M. C.; Jia, S.-L.; Holten, D.; Ondrias, M. R.; Shelnutt, J. A Manuscript in preparation.

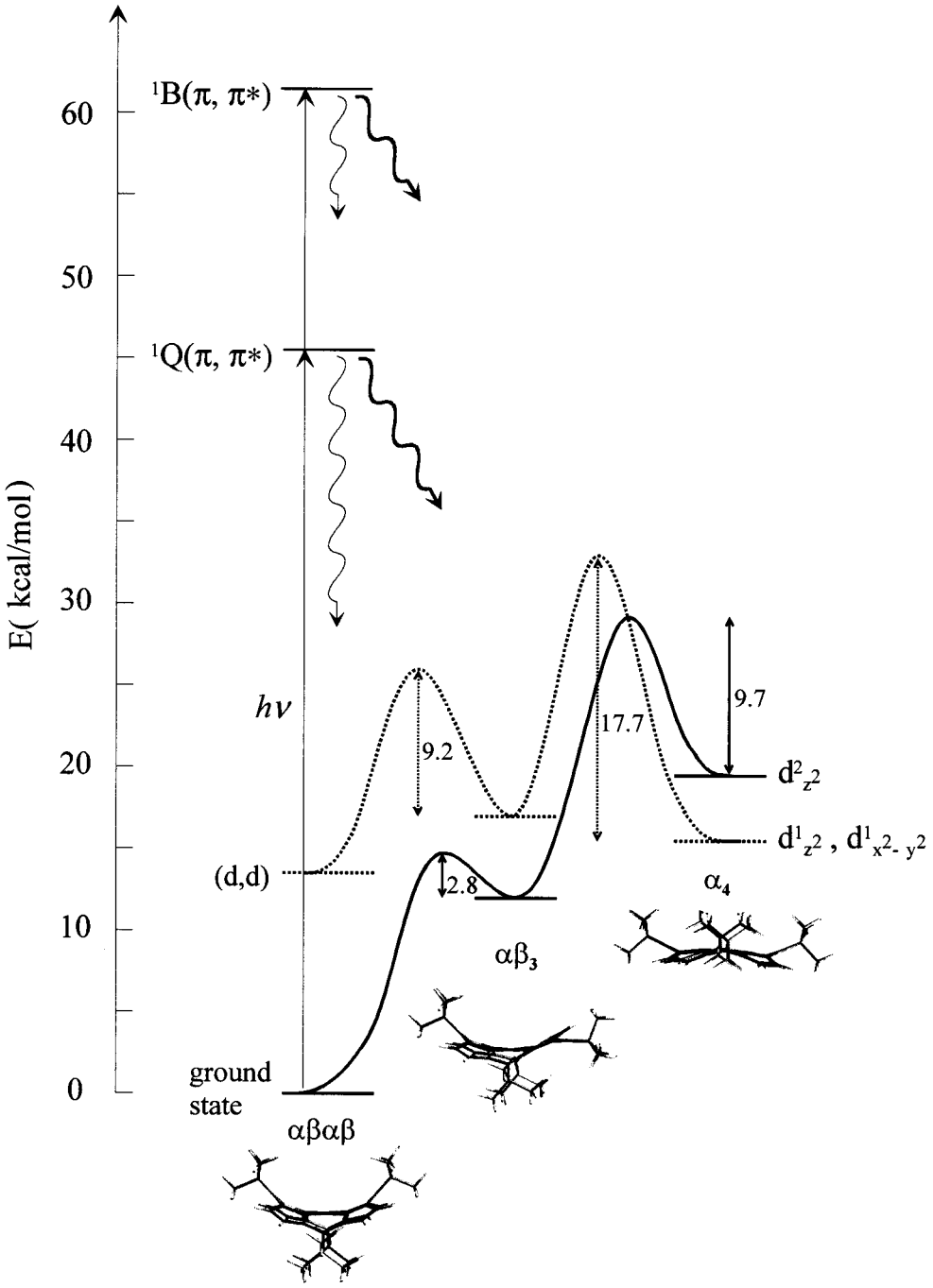

Figure 5. Schematic energy-level diagram for NiT(*t*-Bu)P. The conformational surfaces for the ground state (solid) and the (d,d) excited state (dashed) were obtained from the MM calculations described in the text. The energies of the ^{1}Q(π,π^*) and ^{1}B(π,π^*) states were taken from the ground electronic state absorption spectrum.

a value estimated by modeling the crystal structures of high-spin six-coordinate nickel porphyrins.[5a] For both electronic states and concomitant core sizes, four stable conformers were calculated. In both cases, the lowest-energy conformer is the pure ruffled structure, in agreement with the ground-state X-ray structure[3b] (Figure 5 and Table S1 of the Supporting Information). This conformation (denoted $\alpha\beta\alpha\beta$) has alternating meso-carbons displaced up (α) and down (β) with respect to the mean plane of the macrocycle, causing the pyrrole rings to be twisted clockwise and counterclockwise about the Ni−N bonds. The other stable conformers calculated are the $\alpha\beta_3$, α_4 (dome), and $\alpha_2\beta_2$ (wave) structures, which lie about 12, 20, and 22 kcal/mol, respectively, above $\alpha\beta\alpha\beta$ in the ground electronic state (Figure 5). In the ligand-field state, the $\alpha\beta\alpha\beta$, α_4, and $\alpha\beta_3$ conformers lie within 3 kcal/mol of one another (with the ordering depending on the exact equilibrium Ni−N distance chosen for the d_{z^2},$d_{x^2-y^2}$ metal configuration), with the $\alpha_2\beta_2$ form at somewhat higher energy. The dipole moments estimated for the various stable conformers and the structures at the peaks of the barriers between the stable conformers are listed in Table 4.

INDO/s quantum calculations were performed to supplement the MM calculations. The results are given in Table S2 of the Supporting Information. The calculations lead to several qualitative conclusions. (i) The formation of the (d_{z^2},$d_{x^2-y^2}$) excited state of course favors the expanded-core structures. This is particularly true for $\alpha\beta_3$ and α_4 because these conformers allow large increases in the Ni−N distance relative to the $\alpha\beta\alpha\beta$

Table 4. Dipole Moments of Stable Conformers and Some Transition States between Conformers of NiTtBuP Calculated by Molecular Mechanics (MM) and INDO Methods[a]

		dipole moment (D)	
core structure	conformer	MM	INDO
contracted	$\alpha\beta\alpha\beta$: *ruf*	0.00	0.01
	Barrier 1	0.37	
	$\alpha\beta_3$: *ruf* + *dom* + *wav*	0.48	0.82
	Barrier 2	1.11	
	α_4: *dom*	1.46	0.69
	$\alpha_2\beta_2$: *wav*	0.00	0.00
expanded	$\alpha\beta\alpha\beta$: *ruf*	0.00	0.00
	Barrier1	0.32	
	$\alpha\beta_3$: *ruf* + *dom* + *wav*	0.39	0.87
	Barrier 2	1.02	
	α_4: *dom*	1.24	1.17
	$\alpha_2\beta_2$: *wav*	0.00	0.00

[a] Barriers exist between the $\alpha_2\beta_2$ conformer and the other conformers, but these barrier energies were not calculated. Abbreviations for conformations: *ruf* = ruffled, *dom* = domed, *wav* = waved. An equilibrium Ni−N bond length of 1.855 Å is used for the contracted core of the $(d_{z^2})^2$ nickel configuration. An equilibrium Ni−N bond length of 2.070 Å is used for the expanded core of the $(d_{z^2},d_{x^2-y^2})$ nickel configuration. See Figure 5 and Tables S1 and S2 of the Supporting Information for further results from these calculations.

ground-state confomer (by about 0.16 and 0.20 Å, respectively). In fact, the INDO calculations suggest that the lowest-energy metal configuration may switch from $^1(d_{z2})^2$ to $^3(d_{z^2},d_{x^2-y^2})$ in these two expanded-core conformers. (ii) Structural changes such as formation of the expanded-core $\alpha\beta_3$ or α_4 conformers can explain the observed blue shift in the Soret band of the ligand-field excited state relative to the ground state (Figure 2). (iii) The metal $d_{x^2-y^2}$ orbital mixes with the porphyrin π orbitals, implying that $^{1,3}(d_{z^2},d_{x^2-y^2})$ states contain a small amount of charge transfer (CT) between the metal and the ring. (iv) The lowest ^{1,3}CT states involve electron promotion from a porphyrin π orbital to the metal $d_{x^2-y^2}$ orbital and lie above the $^1(\pi,\pi^*)$ states. (v) In the expanded-core $\alpha\beta\alpha\beta$, $\alpha\beta_3$, and α_4 structures, $^3(d_{z^2},d_{x^2-y^2})$ lies well below $^3(\pi,\pi^*)$ and $^1(d_{z^2},d_{x^2-y^2})$ lies near $^1Q(\pi,\pi^*)$, with the exact positions dependent on the conformer and the value of the β(d) parameter used in the calculation. (vi) The dipole moments for the various conformers are in modest agreement with those obtained from the MM calculations and are listed in Table 4.

Discussion

The lifetime of the ligand-field excited state of NiT(*t*-Bu)P varies from several picoseconds in highly polar media to tens of nanoseconds in nonpolar solvents at room temperature, and increases further to several microseconds in all media near 80 K. This striking dependence of the excited-state deactivation rate of NiT(*t*-Bu)P on solvent dielectric properties and temperature is unprecedented for nickel porphyrins. In fact, this type of behavior is highly unusual for most porphyrinic systems in general except for copper porphyrins (vide infra), but even for these few cases, the lifetime variations are orders of magnitude smaller than observed here for NiT(*t*-Bu)P.

The extraordinary behavior exhibited by NiT(*t*-Bu)P originates from a combination of its highly ruffled ground-state structure along with the interplay among the macrocycle conformations, electronic distribution, and solvent interactions of the photoexcited complex. In particular, a unique structural feature of NiT(*t*-Bu)P is the substantial steric crowding of the peripheral substitutents (Figure 1). These steric constraints limit the ability of this highly ruffled porphyrin to increase its Ni−N distance to accept the large nickel ion in the $(d_{z^2},d_{x^2-y^2})$ configuration generated upon photoexcitation. In other words, the Ni$(d_{x^2-y^2})$−nitrogen electron repulsion in the ligand-field excited state can only be relieved in a limited number of ways. One is for photoexcited NiT(*t*-Bu)P to counteract the strong tendency of a purely ruffled porphyrin for a small metal−nitrogen distance[3,4] by assuming a less distorted but still ruffled $\alpha\beta\alpha\beta$ structure. Another is for electronically excited NiT(*t*-Bu)P to change to a different stable conformer with a less pronounced preference for a short metal−nitrogen distance. These conformers include the α_4 (dome) and $\alpha\beta_3$ (mixed ruffle + dome + wave) structures, which more easily adjust to the electron-density distribution in the (d,d) state because the doming deformation expands the porphyrin core.[4e] (The metal ion moving out of the nitrogen plane may also help reduce the electron repulsion.) Furthermore, the MM calculations indicate that the α_4 and $\alpha\beta_3$ conformers are energetically close to the $\alpha\beta\alpha\beta$ conformer in the (d,d) excited state and are thus accessible following photoexcitation (Figure 5).

The combination of severe steric constraints, a strong preference for a short Ni−N distance in the $\alpha\beta\alpha\beta$ conformer, the need to relieve electron repulsion in the ligand-field excited state, and the limited ways that these factors can be accommodated have profound structural and electronic consequences on the dynamic photophysical behavior of NiT(*t*-Bu)P. One consequence is that the excited-state deactivation of NiT(*t*-Bu)P is over 10^2 slower in nonpolar solvents at room temperature and over 10^4 slower at low temperature than in nominally planar complexes such as NiTPP. These considerations suggest that a kinetic trapping mechanism may apply for NiT(*t*-Bu)P. This behavior probably originates from the formation of a conformer in the ligand-field excited state (e.g., $\alpha\beta_3$ or α_4) that has a poor Franck−Condon factor and large barrier for deactivation to the ruffled ($\alpha\beta\alpha\beta$) ground electronic state. Indeed, the MM calculations indicate that significant barriers toward conformational interconversions exist for NiT(*t*-Bu)P (Figure 5), and that the barrier between the $\alpha\beta_3$ and $\alpha\beta\alpha\beta$ conformers of the ground electronic state is about 3 kcal/mol. This barrier is comparable to the activation enthalpies (1−3 kcal/mol) estimated from the Arrhenius behavior of the deactivation rates (Figure 4).

A second consequence of the combined structural and electronic factors operative in NiT(*t*-Bu)P is that the photoexcited molecule is apparently polar, explaining the observed sensitivity of the excited-state deactivation rate on the dielectric properties of the solvent. Although the $\alpha\beta\alpha\beta$ conformation of the electronic ground state of NiT(*t*-Bu)P is nonpolar, two likely alternate conformations of the ligand-field excited state, namely $\alpha\beta_3$ and α_4, are structurally asymmetric and, hence, polar. The polar character of the photoexcited molecule may be further enhanced if the nominal (d,d) state acquires a small amount of metal-ring CT character (and thus inherent electronic asymmetry). Such CT character can be viewed as arising either from mixing of the metal d and porphyrin π orbitals (indicated in the INDO calculations) or from quantum admixing of a metal-ring CT configuration into the metal $(d_{z^2},d_{x^2-y^2})$ configuration.[23,24]

The MM and INDO calculations indicate that the dipole moments of NiT(*t*-Bu)P in the α_4 and $\alpha\beta_3$ conformers, as well as of the structures at the peaks of the barriers between the stable conformers, are between 0.3 and 1.5 D (Table 4). These values are comparable in magnitude to the dipole moments of the solvents in which the molecule was studied (Table 1).[25] Hence, the energies of the various conformers in both the excited and ground electronic states will change with respect to one another

as a function of solvent polarity. The reorganization energies will also differ due to the stronger interaction of the porphyrin dipoles with the polar solvents. These factors will modulate the excited-state deactivation rate as the dielectric properties of the solvent are varied. This solvent dependence will occur through changes in the relationships (curve crossings) between the ground and excited-state potential energy surfaces (reflecting both internal porphyrin coordinates and solvent coordinates) and changes in the relevant barriers toward conformational interconversions and solvent reorganizations on both surfaces. Furthermore, the extent of solvent reorganization and the associated stabilization of the polar excited-state conformations will diminish as the temperature is lowered. These effects, as well as the reduced ability for the molecule to surmount any associated barriers, should contribute to the slowing of the excited-state deactivation as the temperature is lowered and to the similar rates observed in polar and nonpolar media near 80 K.

The properties of the medium and the effects of temperature may affect not only the rate of deactivation of a given conformer of the (d,d) excited state, but also the type of (d,d) conformer that is initially produced. Previous results (including large absorption/fluorescence shifts) for H_2T(*t*-Bu)P and ZnT(*t*-Bu)P, and for other nonplanar free-base and zinc porphyrins, suggest that these molecules undergo photoinduced structural changes in the $^1(\pi,\pi^*)$ excited state.[6,7a,b] The same would be expected to be true for NiT(*t*-Bu)P as well. Furthermore, the different dielectric properties of the solvent, or specific interactions of the macrocycle or metal with the solvents in list B, may help direct or limit the (π,π^*) decay to specific molecular structures of the ligand-field state (e.g., $\alpha\beta\alpha\beta$, $\alpha\beta_3$, or α_4). Such directing toward specific stable conformers by solvent and temperature may also occur within the initially formed and vibrationally unrelaxed (d,d) excited state. Additionally, environmental effects could also control whether the decay proceeds predominantly in the singlet manifold [i.e. $^1(\pi,\pi^*) \rightarrow {}^1$(d,d) $\rightarrow$ ground state], or whether it involves intersystem crossing to the ^{3}(d,d) state; this issue is unresolved even for planar nickel porphyrins.[8] However, it is unclear that changes in the overall conformation or multiplicity of the ligand-field state as a function of solvent or temperature uniquely determine the following observations: (i) the single-exponential decay of the (d,d) excited state under all conditions, (ii) the very modest differences in the transient spectra of the excited states induced by different solvents and temperatures, and (iii) the smooth (continuous) variations in the excited-state decay time with solvent dielectric and temperature. However, the observed time-resolved optical data are clearly *not* consistent with the conversion of the transient state from a (d,d) state to the $^3(\pi,\pi^*)$ state as the solvents or temperatures are varied.

Nonplanar distortions may play a significant role in the photophysical properties of NiT(*t*-Bu)P not simply from a static but also from a dynamic point of view. In particular, the out-of-plane modes (ruffling, saddling, doming, etc) that are almost certainly involved in the conformational interconversions have low energies ($20-50$ cm^{-1})[5a] and are thus populated well above the zero point at room temperature. Anharmonic coupling of these modes with the in-plane vibrations could affect the pathways and rates of vibrational-energy redistribution and relaxation in the (d,d) state and thus the ultimate conformation of the ligand-field excited state. These out-of-plane modes also may facilitate mixing of the CT and (d,d) states. Such vibration-induced modulation of the electronic character of the photoexcited porphyrin (Born−Oppenheimer breakdown) would provide an additional mechanism for excited-state deactivation. Similarly, the out-of-plane motions likely play a similar role in the excited-state dynamics of the free-base and zinc analogues, H_2T(*t*-Bu)P and ZnT(*t*-Bu)P.[6b,c]

Finally, it should be noted that the ideas discussed here to understand the photodynamics of NiT(*t*-Bu)P and NiT(Ad)P also may be relevant to the deactivation behavior observed for copper(II) porphyrins such as CuOEP and CuTPP. Due to the presence of the unpaired $d_{x^2-y^2}$ metal electron, the lowest excited $^3(\pi,\pi^*)$ state of the macrocycle splits into $^2(\pi,\pi^*)$ and $^4(\pi,\pi^*)$ states, referred to as the "tripdoublet" and the "quartet" states.[26a] The involvement of a ring-$\pi \rightarrow$ metal-$d_{x^2-y^2}$ CT state or the $(d_{z^2},d_{x^2-y^2})$ state, photoinduced nonplanar distortions, and a combination of these have been invoked to explain the dependence of the spectral properties and decay times of the $^{2,4}(\pi,\pi^*)$ states on solvent polarity (*i.e.*, 100 ns in CH_2Cl_2 to 1 μs in pentane for CuOEP[26c]), temperature, viscosity, macrocycle, and metal-coordination state.[26] In particular, as in the present situation for NiT(*t*-Bu)P, the excited-state deactivation times of the copper porphyrins appear to be strongly influenced by the involvement of excited states whose energies and properties are modulated by the interplay between the electron density distribution in the porphyrin (including the population of the metal $d_{x^2-y^2}$ orbital) and static/dynamic distortions of the macrocycle.

Conclusions

The excited-state relaxation dynamics of NiT(*t*-Bu)P exhibit a dependence on solvent dielectric properties and temperature

(23) It should be noted, however, that transient optical data and the INDO calculations are inconsistent with a pure CT state being the lowest excited state of NiT(*t*-Bu)P and giving rise to the observed spectral and kinetic behavior. A CT state involves a shift of electron density between the metal and the macrocycle, formally producing $Ni^{III}P^-$ or $Ni^{I}P^+$. The INDO calculations (see Supporting Information) suggest that the lowest of these states lies well above the $^1(\pi,\pi^*)$ states and thus could not lie directly along the deactivation pathway of the photoexcited molecule. More directly, the observed kinetic and spectral behavior of NiT(*t*-Bu)P and NiT(Ad)P are inconsistent with such a CT state being one of the observed transient states. Such a state would show a pronounced dependence of the transient Soret band on solvent polarity (much larger than is observed) and the transient spectra would exhibit broad porphyrin cation- or anion-like absorption to the red of 600 nm (Felton, R. H. In *The Porphyrins*; Dolphin, D., Ed.; Academic Press: New York, 1978; Vol. III, p 1). The latter absorption characteristics are not observed.

(24) The INDO calculations suggest that the lowest CT configuration involves movement of charge from a porphyrin π HOMO to the empty metal $d_{x^2-y^2}$ orbital. Mixing with the (d_{z2}, d_{x2-y2}) configuration would not only increase the electronic asymmetry due to the charge distribution inherent in the CT state but would also reinforce the structural and electronic effects arising from population of the metal $d_{x^2-y^2}$ orbital. Of course, this is but one example, and the introduction of a small amount of metal-ring CT character of any type would have a significant effect on the electronic asymmetry and hence polarity of photoexcited NiT(*t*-Bu)P.

(25) Of course, the polarity of photoexcited NiT(*t*-Bu)P may contain contributions not only from the dipole moments, but also from the quadrupole moments of the relevant conformers.

(26) (a) Gouterman, M. In *The Porphyrins*; Dolphin, D., Ed.; Academic Press: New York, 1978; Vol. V, p 53. (b) Antipas, A.; Dolphin, D.; Gouterman, M.; Johnson, E. C. *J. Am. Chem. Soc.* **1978**, *100*, 7705. (c) Kim, D.; Holten, D.; Gouterman, M. *J. Am. Chem. Soc.* **1984**, *106*, 2793. (d) Shelnutt, J. A.; Straub, K. D.; Rentzepis, P. M.; Gouterman, M.; Davidson, E. R. *Biochemistry* **1984**, *23*, 3946. (e) Yan, X.; Holten, D. *J. Phys. Chem.* **1988**, *92*, 5982. (f) Asano, M.; Kaizu, Y.; Kobayashi, H. J. *J. Phys. Chem.* **1988**, *89*, 6567. (g) Lie, F.; Cunningham, K. L.; Uphues, W.; Fink, G. W.; Schmolt, J.; McMillen, D. R. *Inorg. Chem.* **1995**, *34*, 2015. (h) Kruglik, S. G.; Apanasevich, P. A.; Chirvonyi, V. S.; Kvach, V. V.; Orlovich, V. A. *J. Phys. Chem.* **1995**, *99*, 2978. (i) DePaula, J. C.; Walters, V. A.; Jackson, B. A.; Cardozo, K. P. *J. Phys. Chem.* **1995**, *99*, 4373. (j) Jeoung, S. C.; Kim, D.; Cho, D. W.; Yoon, M. *J. Phys. Chem.* **1995**, *99*, 5826. (k) Asano-Someda, M.; Kaizu, Y. *J. Photochem. Photobiol. A (Chem.)* **1995**, *87*, 23. (l) Cunningham, K. L.; McNett, K. M.; Pierce, R. A.; Davis, K. A.; Harris, H. H.; Falck, D. M.; McMillen, D. R. *Inorg. Chem.* **1997**, *36*, 608.

whose magnitude is unprecedented for porphyrinic systems (picoseconds to microseconds). The dramatic dependence of the excited-state deactivation on environmental factors is most readily understood if the photoexcited molecule is polar because it possesses an asymmetric structure, inherent electronic asymmetry (i.e., metal-ring CT character), or both. The low-frequency out-of-plane vibrations of the macrocycle may be intimately involved in the overall excited-state decay and ground-state recovery process.

Clearly both the solvent and temperature dependence of the excited-state relaxation of NiT(*t*-Bu)P and NiT(Ad)P ultimately derive from the profound effects that static and dynamic nonplanar distortions have on the (photo)physical and chemical properties of porphyrinic chromophores. The wide range of excited-state kinetic behavior and other chemical properties accessible through conformational "tuning" may well mimic a strategy used in biological systems to modulate the reactivity of porphyrinic prosthetic groups, which are increasingly found to be nonplanar in the crystal structures of tetrapyrrole−protein complexes.[2] Furthermore, the work reported here on NiT(*t*-Bu)P may provide additional clues to the interactions between a tetrapyrrolic cofactor and the surrounding protein. For example, the likelihood that certain types of nonplanar porphyrin distortions impart some (albeit small) polar character to the molecule may be relevant to the transient dynamics in hemoglobin and myoglobin. In particular, the transient polar character of the domed heme intermediates known to form in these systems[27] could contribute to the protein response elicited by ligand binding/release at the active site. In addition to the potential relevance to tetrapyrrole−protein complexes, the dependence of the excited-state dynamics of NiT(*t*-Bu)P on solvent dielectric properties might also find use in optical-switching applications. In general, the accessibility of a wide range of excited-state properties in nonplanar porphyrins may afford simple avenues into useful building blocks for molecular optoelectronics devices.

Acknowledgment. This work was supported by grants from the National Institutes of Health (GM34685 to D.H.), National Science Foundation (CHE-96-23117 to K.M.S), and the Division of Chemical Sciences, U.S. Department of Energy, under Contract DE-AC02-76CH00016 (to J.F.). Sandia is a multiprogram laboratory operated by Sandia Corporation, a Lockheed Martin Company, for the United States Department of Energy under Contract DE-AC04-94AL85000 (to J.A.S.). M.C.S. was supported by a Department of Energy Distinguished Postdoctoral Research Fellowship.

Supporting Information Available: Figures illustrating the isosbestic behavior observed for the decay of the (d,d) excited state and the relationship of the excited-state lifetime and the (π,π*)/(d,d) Soret-region absorbance-change ratio, as well as tables containing the results of the MM and INDO calculations (6 pages, print/PDF). See any current masthead page for ordering information and Web access instructions.

JA974101H

(27) (a) *The Iron Porphyrins*; Gray, H. B., Lever, A. B. P., Eds; Addison Wessley: London, 1983. (b) Zhu, L.; Sage, J. T.; Champion, P. M. *Science*, **266**, *629*, 1994. (c) Jentzen, W.; Ma, J.-G.; Shelnutt, J. A. *Biophys. J.* **1988**, *74*, 753.